Onset temperature for the Kosterlitz-Thouless transition in the $\nu_t = 1$ bilayer quantum Hall state

D. Terasawa* and A. Fukuda
Department of Physics, Hyogo College of Medicine, Nishinomiya 663-8501, Japan

T. Morikawa
Graduate School of Science, Department of Physics, Kyoto University, Kyoto 606-8502, Japan

Y. D. Zheng and A. Sawada
Research Center for Low Temperature and Materials Sciences, Kyoto University, Kyoto 606-8501, Japan

Z. F. Ezawa
Advanced Meson Science Laboratory, Riken, Wako 980-8578, Japan

(Received 19 July 2012; published 19 October 2012)

We investigate the onset temperature T^* of the bilayer quantum Hall state at the total Landau level filling factor $\nu_t = 1$ together with the activation energy gap Δ. The onset temperature is the temperature at which the quantum Hall state starts to form. We make two remarkable experimental observations: (1) As the total electron density decreases, T^* increases while Δ decreases on account of the deterioration of electron mobility. (2) As the in-plane magnetic field increases, T^* exhibits a rise at the point where Δ becomes a minimum. The minimum of Δ occurs at the transition point from the commensurate phase to the recently discovered soliton lattice phase. We discuss the relation between T^* and the Kosterlitz-Thouless transition on the basis of the XY symmetry possessed by the $\nu_t = 1$ bilayer system and discuss the experimentally observed behavior of T^*.

DOI: 10.1103/PhysRevB.86.165320 PACS number(s): 73.43.−f, 64.70.Tg

I. INTRODUCTION

Bilayer quantum Hall states (BQHSs) are one of the most interesting systems observed in condensed matter physics in which correlated electrons exhibit a rich variety of phenomena.[1,2] In particular, the interest generated in the BQHS at the total Landau level filling factor $\nu_t = 1$ has encouraged numerous theoretical and experimental studies because the layer degree of freedom in this quantum Hall state demonstrates the fundamental aspects of electron correlations. Recently, the prospects of realizing exciton superfluidity[3,4] and Josephson tunneling currents[5–8] in two separately contacted two-dimensional electron gases (2DEGs) have fueled renewed research into the formation of the BQHS in GaAs/AlGaAs heterostructures.

In the bilayer system, the layer degree of freedom can be described as a pseudospin by equating the "up" ("down") pseudospins with electrons in the upper (lower) layer. The layer separation causes the pseudospins to align along the XY plane to minimize the capacitive charging energy, and thus the system possesses an easy-plane anisotropy. One of the important aspects of a system with XY symmetry is the possibility of the system manifesting the finite-temperature Kosterlitz-Thouless (KT) transition.[8] For the $\nu_t = 1$ BQHS, two cases of KT transition can be considered theoretically.[9–13]

The first case of KT transition is when the energy gap between the symmetric and antisymmetric wave functions, Δ_{SAS}, which is known as the tunneling energy, equals zero. In this case, the pseudospins spontaneously break the symmetry and lead to the formation of an itinerant XY ferromagnet. The state possesses pseudospin vortex excitations (merons), and they form vortex-pairs (bimerons) below the KT transition temperature T_{KT}. The KT transition occurs when a vortex-pair is dissociated into two free vortices at T_{KT}, because a free vortex destroys the long-range order of the system.[9,10,12]

The second case of KT transition is observed in the recently discovered soliton-lattice (SL) phase.[14,15] When an in-plane magnetic field $B_\parallel$ is applied to the BQHS with a nonzero tunneling gap ($\Delta_{SAS} \neq 0$), the system undergoes a transition[9] from the commensurate (C) phase to the incommensurate (IC) phase as a result of the competition between the exchange energy ($\propto \rho_{ps}$) and the tunneling energy ($\propto \Delta_{SAS}$). Here, ρ_{ps} denotes the pseudospin stiffness that originates in the interlayer Coulomb exchange energy [see Eq. (3) in Sec. IV A]. Experimentally, this transition was first discovered by Murphy *et al.*[16] when they observed that the activation energy gap Δ changed its behavior from a rapid decrease to saturation at a constant value. The SL phase exists at the C-IC transition point, and it is manifested by the occurrence of a highly anisotropic transport[14] and a downward cusp in Δ.[15] The SL is composed of quantized magnetic vortices in a manner similar to those observed in a Josephson junction, where each vortex represents a 2π twist in the interlayer phase. In the SL phase, the translational symmetry of the XY ferromagnet is restored, and KT transition is induced by the dislocation-mediated melting of the SL.[9,11,13] An important feature is that, since the bimerons and dislocations in the SL are electrically charged, the KT transition can be detected by magnetotransport experiments.

Lay *et al.*[17] noticed an interesting aspect of the onset temperature T^*, the temperature below which the quantum Hall state (QHS) starts to form (see Fig. 1), by using a wide-quantum-well sample. Their data showed a peculiar result that, even when Δ was constant, T^* decreased as the electron density n_t increased. That is, paradoxically, the two quantities showed different dependencies on n_t. Lay *et al.* suggested the relation between T^* and T_{KT} because, in their experiment, the behavior of T^* was not inconsistent with the theoretical prediction made for the behavior of T_{KT}.[9] In a later study, Abolfath *et al.*[18] discussed the above result based on the

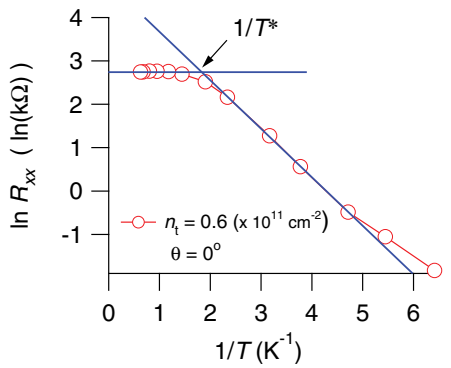

FIG. 1. (Color online) Graphical representation of parameters T^* and Δ. The temperature at which the activated behavior terminates is marked by T^*.

reduction in ρ_{ps} with an increase in n_t. However, although the large Δ_{SAS} of their sample decreased with increasing n_t, its effect on T^* was not analyzed. Furthermore, no experiments have thus far investigated the behavior of T^* for the SL phase.

In this study, we investigate the dependence of T^* on n_t and $B_\parallel$ in the $\nu_t = 1$ BQHS with small Δ_{SAS} sample. The dependence of T^* on n_t shows a behavior similar to that observed by Lay *et al.*[17] This behavior is well explained by the reduction in the pseudospin stiffness ρ_{ps}, as mentioned previously, whereas Δ decreases due to the decrease of the electron mobility in the low-density regime. As regards the $B_\parallel$ dependence, Δ decreases rapidly with increasing $B_\parallel$ up to the transition point, whereas T^* remains almost constant both in the C and IC phases except in the region immediately after the transition point (i.e., over the SL phase). These results indicate that the behaviors of Δ and T^* are not correlated and that T^* has a distinctive dependence on n_t and $B_\parallel$. We discuss the physical interpretation of T^* in the context of the KT transition, and we observe a reasonable agreement of our results with theoretical predictions.

This paper is consisted as follows: In Sec. II, the experimental method is described. In Sec. III, we present the experimental results regarding the variation in Δ and T^*, after defining Δ and T^*. First we examine their n_t dependence and then $B_\parallel$ dependence. In Sec. IV, we discuss our results by comparing them with the KT transition based on the bimeron separation model (for n_t dependence) and the SL melting model (for $B_\parallel$ dependence). Finally, we present the summary in Sec. V.

II. EXPERIMENT

The sample used in this study, which was grown at the NTT Basic Research Laboratories, consists of two 20-nm-wide GaAs quantum wells separated by a 3-nm-wide AlAs barrier layer; thus, the actual separation d between the two 2DEGs is 23 nm. The estimated value of Δ_{SAS} of this sample is approximately 1 K. Experiments are carried out at the balanced density point by varying n_t. We can independently control the electron density in each layer[19] by adjusting the front- and back-gate biases while maintaining the densities of the two layers as equal. The sample is mounted in the mixing chamber of a dilution refrigerator at a base temperature of 40 mK. Measurements are performed using a standard low-frequency (=17.7 Hz) ac lock-in technique with a current of 10 nA. The in-plane field $B_\parallel$ is applied by tilting the sample within the magnetic field B_t using a goniometer with a superconducting stepper motor.[20] The tilting angle θ is expressed by $B_\parallel/B_\perp = \tan\theta$, where $B_\perp$ denotes the perpendicular component of the applied B_t to the 2DEG plane. Recall that the Landau quantization of a 2DEG is determined by $B_\perp$.

III. RESULTS

First, we provide the definitions of Δ and T^* in the context of our study. Figure 1 shows a typical Arrhenius plot (the inverse temperature $1/T$ dependence of the longitudinal resistance R_{xx}) of the $\nu_t = 1$ BQHS. The excitation gap Δ is determined from the expression $\ln(R_{xx}) = \ln(R_0) - \Delta/(2T)$. In this experiment, we carefully fit the slope in order to realize the maximum value of $\partial \ln(R_{xx})/\partial(1/T)$, and thus, an appropriate value of Δ. The onset temperature T^* is determined by the crossover point of R_{xx} from the low-temperature activated transport regime to the high-temperature saturated resistance regime, following the approach of Lay *et al.*[17] Above T^*, the R_{xx} minimum at $\nu_t = 1$ vanishes and R_{xx} is almost independent of T and $B_\perp$. We deduce T^* from the relation $1/T^* = [(\ln(R_{sat}) - \ln(R_0)]/(-\Delta/2)$, where R_{sat} represents the saturated R_{xx} value in the high-temperature limit. In general, any disorder present in the sample always causes the ideal sharp transition to be converted into a crossover transition from the low-temperature activated regime to the high-temperature saturated R_{xx} regime, as we see in the plot. Nevertheless, the obtained values are not significantly different from the ideal values.

Figure 2 shows the observed values of Δ and T^* as a function of n_t at $\theta = 0$ ($B_\parallel = 0$). It is found that Δ becomes maximum around $n_t = 0.7 \times 10^{11}$ cm^{-2}, and then it decreases to zero (non-QHS) as n_t increases. This decrease occurs because the *intralayer* Coulomb energy overcomes the *interlayer* Coulomb energy.[16] When n_t increases, there is an increase in the ratio of the intralayer Coulomb interaction to the

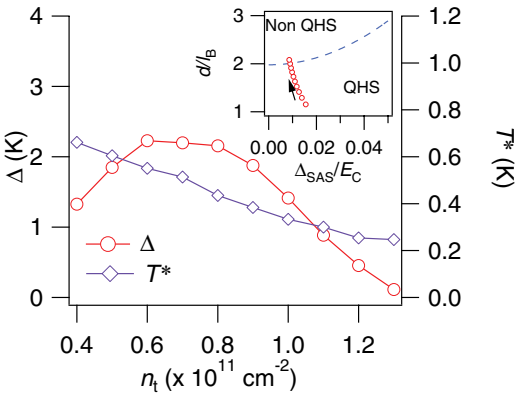

FIG. 2. (Color online) Plots of Δ (left axis) and T^* (right axis) as a function of n_t. Inset: The zero-temperature phase diagram of the $\nu = 1$ bilayer system at $B_\parallel = 0$. E_C represents the Coulomb energy [$=e^2/(\epsilon\ell_B)$, e denotes the elementary charge and ϵ denotes the dielectric constant]. The circles indicate the phase positions corresponding to the data and the arrow indicates the direction in which n_t increases.

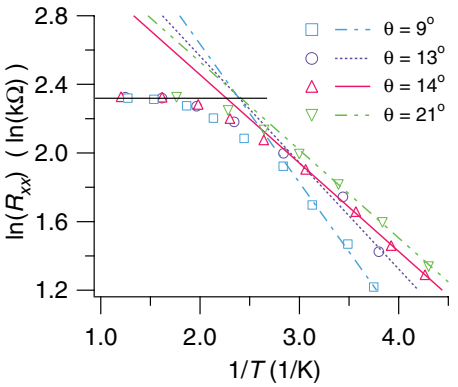

FIG. 3. (Color online) Arrhenius plot ($\ln R_{xx}$ versus $1/T$) for several values of θ at $n_t = 0.8 \times 10^{11}$ cm^{-2}.

interlayer Coulomb interaction, which is usually expressed as d/ℓ_B, with $\ell_B \equiv \sqrt{\hbar/(eB_\perp)}$ denoting the magnetic length. In the high-n_t regime, the system approaches a system consisting of two individual 2DEGs with each of the layers having a filling fraction of 1/2 [Refs. 21,22] (see the phase position in the inset phase diagram). This system essentially corresponds to two composite Fermion metal states,[22,23] and hence to a compressible state. On the other hand, the decrease in Δ in the low-n_t regime is due to the deterioration of electron mobility.[24] In contrast to the Δ behavior, T^* shows a monotonic decrease as n_t increases, similar to the result in Ref. 17.

Subsequently, we apply the in-plane field $B_\parallel$ to our sample to investigate the behavior of Δ and T^* in the SL phase. Figure 3 shows the Arrhenius plot for several values of θ at $n_t = 0.8 \times 10^{11}$ cm^{-2}. The slopes used to determine Δ and the crossing points used to determine T^* are also shown. As the sample is tilted within the magnetic field, Δ decreases as the tilt angle increases; however, the activated regions start to form at almost the same temperature. On the other hand, we observe that only the crossing point $(1/T^*)$ at $\theta = 14^\circ$ slightly shifts to the left (to a higher temperature) when compared with the three remaining crossing points, even though the slopes of Arrhenius plots for $\theta = 14^\circ$ and $\theta = 21^\circ$ are nearly identical. We also observe a similar shift in the slopes for the sample with $\Delta_{SAS} \sim 11$ K (not shown here). For $T > T^*$, R_{xx} becomes independent of T as well as the $B_\parallel = 0$ cases.

Figure 4 shows Δ and T^* as a function of θ for two different values of n_t. At $n_t = 0.8 \times 10^{11}$ cm^{-2}, Δ shows a behavior that is typical of the C-IC transition. We observe a small dip at the transition point, which indicates the formation of the SL phase in this sample with a small Δ_{SAS}. On the contrary, T^* is almost constant over the measured region of θ except for a clear rise observed immediately after the transition point, at which the SL phase begins to form. This feature of T^* is somewhat unexpected in two aspects: (1) T^* does not decrease with increasing θ although Δ decreases to about half of its initial value until the C-IC transition occurs. This suggests that T^* is not affected by the activation energy gap Δ and that it has a distinctive dependence on $B_\parallel$, at least in the $\nu_t = 1$ BQHS. (2) Although the system is rather unstable at the transition point, T^* shows an increase in this region, thereby indicating that the BQHS begins to form at higher temperatures than the C phase. The two above-mentioned points can appear

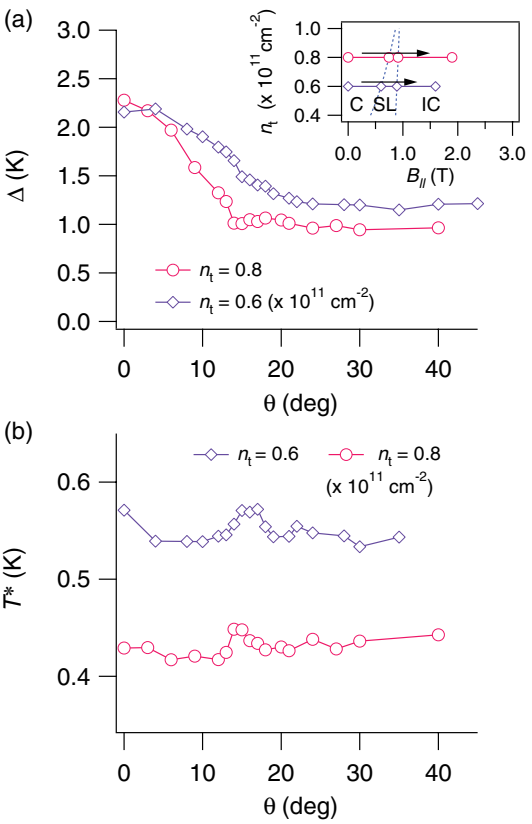

FIG. 4. (Color online) (a) Δ and (b) T^* as a function of θ for $n_t = 0.6$ and 0.8×10^{11} cm^{-2}. Inset: The zero-temperature phase diagram at the $\nu_t = 1$ bilayer QHS in the n_t versus $B_\parallel$ plane. The points shown correspond to the experimental regions to which $B_\parallel$ is applied.

counterintuitive because we can intuitively perceive that the state with a smaller Δ would require lower temperatures to begin to form a QHS.

Another interesting aspect of the behavior of Δ for $n_t = 0.6 \times 10^{11}$ cm^{-2} is that Δ does not show a definite C-IC transition point although T^* exhibits a clear rise at $\theta = 14^\circ$. With regard to the transition point, it is necessary to study the R_{xx} behavior at low values of T. Figure 5 shows the variation in R_{xx} at $T \approx 110$ mK for $n_t = 0.6$ and 0.8×10^{11} cm^{-2} as a function of θ. We notice that R_{xx} for both densities rises

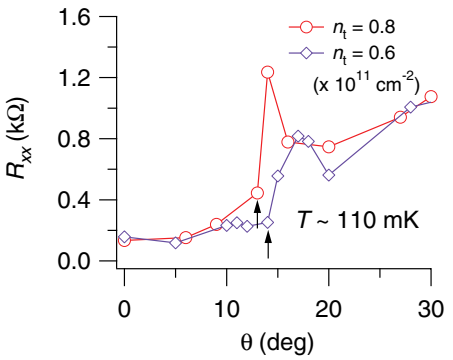

FIG. 5. (Color online) R_{xx} at $T \sim 110$ mK as a function of θ for $n_t = 0.6$ and 0.8×10^{11} cm^{-2}. The arrows indicate the transition points.

abruptly (indicated by arrows). The sudden rise is the sign of the onset of the SL phase,[15] since the dissipation occurs due to the scattering of charged carriers by the SL.[25] Hence, we can conclude that the SL phase starts to form at $\theta = 14^\circ$ for $n_t = 0.6$ and at $\theta = 13^\circ$ for $n_t = 0.8 \times 10^{11}$ cm^{-2}.

The reason that the C-IC transition point is not apparent in the behavior of Δ remains unclear; however, we speculate that certain disorder effects may be the underlying cause. We recall[1] that the tunneling energy density is given by

$$\mathcal{E} = -\tfrac{1}{2} n_t \Delta_{SAS} \cos[\theta(x) - \delta_m x], \quad (1)$$

with $\delta_m \equiv edB_\parallel/\hbar$, where θ represents the interlayer phase field. Furthermore, we recall that the SL is described by a periodic solution of the sine-Gordon equation,

$$\rho_{ps}\partial_x^2\theta - \tfrac{1}{2} n_t \Delta_{SAS} \sin[\theta(x) - \delta_m x] = 0. \quad (2)$$

These equations indicate that the soliton is stabilized by the tunneling energy $\mathcal{E}$, which is proportional to the total density n_t and the tunneling gap Δ_{SAS}. Hence, we can conclude that the SL will show greater stability in samples with larger values of $n_t\Delta_{SAS}$. This is consistent with the experimental observation of a clear cusp that appears in Δ at the C-IC transition point, where the SL develops, in the sample with $\Delta_{SAS} \sim 11$ K. In contrast, when $n_t\Delta_{SAS}$ is extremely small, the tunneling energy may be overcome by the energy associated with disorder. We can ascribe the origin of the disorder to randomness in the tunneling by impurities or small variations in the barrier thickness. The disorder may also arise simply due to spatial variations in densities that can change the C-IC transition point locally. In any case, a well-developed SL would not appear since it is unstable when $n_t\Delta_{SAS}$ is too small.

IV. DISCUSSION

A. T^* and bimeron separation

From Fig. 2, it can be observed that the onset temperature T^* decreases as n_t increases or, equivalently, as d/ℓ_B increases. We now relate this unique behavior of T^* to that of the KT transition temperature T_{KT}. It has been argued[9] that, if $\Delta_{SAS} = 0$, the separation of a bimeron induces the KT transition at $T_{KT} = (\pi/2)\rho_{ps}$. The pseudospin stiffness ρ_{ps} is given by the Hartree-Fock approximation as

$$\rho_{ps} = \frac{e^2}{16\pi\epsilon\ell_B}\int_0^\infty dx x^2 \exp[-x^2/2 - xd/\ell_B], \quad (3)$$

where e denotes the elementary charge and ϵ denotes the dielectric constant. It is clear from this formula that ρ_{ps} decreases as d/ℓ_B increases, because ρ_{ps} is attributed to the interlayer Coulomb exchange interaction that decreases with increasing d/ℓ_B. The manifestation of the KT transition in the electric transport experiment is not entirely clear, although it is argued that R_{xx} is almost independent of T and $B_\perp$ for $T \geqslant T_{KT}$ and displays an activated dependence on T for $T < T_{KT}$ because, unlike in other cases,[26] the paired vortices have an electrical charge e while their vorticity is neutral in the temperature range below T_{KT}.[10] Above T_{KT}, free vortices destroy the long-range order of the QHS and thus the system becomes a compressible state.

Figure 6 shows the plot of the observed T^* together with the calculated T_{KT} as a function of d/ℓ_B. As observed,

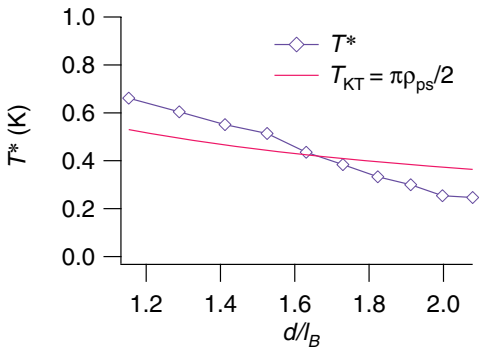

FIG. 6. (Color online) Plot of T^* as a function of d/ℓ_B along with the curve for T_{KT} that follows the equation $T_{KT} = \pi\rho_{ps}/2$.

the experimental T^* curve and the calculated T_{KT} curve show good agreement without the application of any fitting parameters. Thus, even for low values of n_t, the behavior of T^* demonstrates the intrinsic property of the interlayer Coulomb correlation effect without being affected by the reduction in electron mobility. Our result shows a better agreement with the theoretical values than the previous work,[17] probably due to the smaller Δ_{SAS} of our sample. Hence, our result indicates that the KT transition, as elucidated by the bimeron separation model, can explain the behavior of T^* very well. The deviations at small and large d/ℓ_B values may originate due to the nonzero Δ_{SAS} value of the sample that reduces with increasing d/ℓ_B.

B. T^* and soliton-lattice melting

In order to examine the $B_\parallel$ dependence of T^*, we again discuss the behavior of T^* with reference to the KT transition. Let us review the two points raised in Sect. III: (1) T^* is almost constant, even though Δ decreases rapidly toward the C-IC transition point; (2) T^* shows a clear rise at the C-IC transition point. As regards the first point, the system is in the C phase ($\Delta_{SAS} \neq 0$, $B_\parallel < B_\parallel^c$), and it has been previously argued that the KT transition is eliminated in this case.[9,12] In this state, the bimeron excitation is stretched in the direction of $B_\parallel$.[12] However, it is to be noted that the behavior of T^* can be easily explained if we identify it as T_{KT}. Indeed, it is obvious from Eq. (3) that T_{KT} ($= \pi\rho_{ps}/2$) is independent of $B_\parallel$. However, more theoretical considerations are required for this issue.

The second point mentioned above is of greater significance to this study. To discuss this point, we further investigate the properties of the SL. The observed increase in T^* over the SL phase region indicates that the SL is robust to the increase in T, although the result of Δ indicates that the system loses its ferromagnetic order at temperatures lower than that of the C phase. This phenomenon may be explained as follows: After the transition, solitons proliferate rapidly throughout the sample,[1,13,15] and at a finite temperature the soliton lines begin to meander.[27,28] Hence, the meandering solitons can produce random dissipations of electrons, resulting in the increase in R_{xx} and the reduction in Δ.[15] Furthermore, the solitons themselves have a finite melting or dislocation temperature that is dependent on their elastic properties. The complete melting of the SL should occur at $T = T^*$, above which R_{xx}

is saturated. When $T \geqslant T^*$, the order of the system is again destroyed. The rise in T^* at the C-IC transition point suggests that the KT transition changes to the melting of the SL.

There are several theoretical studies on T_{KT} behavior with regard to the SL.[11,13,29,30] Herein, we compare our experimental results to the results of one of the theories of KT transition in the SL phase. As mentioned previously, for the case $\Delta_{SAS} \neq 0$ and $B_\parallel > B_\parallel^c$, the finite-temperature KT transition can be ascribed to the dislocation-mediated SL melting. Read[11] has argued that the T_{KT} behavior after the transition $B_\parallel > B_\parallel^c$ can be expressed by

$$T_{KT} \sim (K_{11}K_{22})^{1/2} \sim (B_\parallel - B_\parallel^c)^{1/2} \ln^{3/2}[1/(B_\parallel - B_\parallel^c)], \quad (4)$$

where K_{11} denotes the compressional elastic constant and K_{22} denotes the shear elastic constant of solitons. It is to be noted that $K_{11} \propto (B_\parallel - B_\parallel^c)\ln^2[1/(B_\parallel - B_\parallel^c)]$ because an elongated soliton line that is weakly repulsive at the both ends can easily be compressed, while $K_{22} \propto \ln[1/(B_\parallel - B_\parallel^c)]$ because the tilt of a soliton line, where the ground-state energy is minimized when solitons are aligned in the direction of $B_\parallel$, causes a large energy expenditure [see Fig. 7(a)]. For $B_\parallel \to \infty$, the distance between the solitons is extremely small, whereby the ground state becomes completely incommensurate (i.e., the system is well approximated by the isotropic XY model). Hence, both K_{11} and K_{22} approach ρ_{ps}, thereby resulting in $T_{KT} \to \rho_{ps}$. Figures 7(b) and 7(c) display the fitting results for $n_t = 0.6$ and 0.8×10^{11} cm^{-2}, respectively. In order to proceed with the fitting, we use the following formula with two fitting parameters A and C:

$$F(x) = A(B_\parallel - B_\parallel^c)^{1/2} \ln^{3/2}[1/(B_\parallel - B_\parallel^c)] + C. \quad (5)$$

The constant A primarily accounts for the ρ_{ps} term whereas C does not exist in Eq. (4). It is naively considered that disorder modifies the KT temperature to some extent. As we can see, both the T^* values, obtained for $n_t = 0.6$ and 0.8×10^{11} cm^{-2}, are fit very well by Eq. (5) in the SL-phase regime, and then the obtained values deviate from the fitting curve as $B_\parallel$ increases. Although the experimental regions to which $B_\parallel$ is applied in this study remain small, this change is exactly consistent with Read's argument. This further corroborates the equating of T^* with T_{KT}.

Another possible explanation for the behavior of T^*, as given by Lay *et al.*,[17] is that there is a transition from the correlated incompressible BQHS to the uncorrelated compressible Fermi liquid. However, this explanation does not account for the remarkable $B_\parallel$ dependence of the SL phase, because the transition to a compressible state is dependent on the ratio d/ℓ_B. Furthermore, we stress the fact that, in the off-balanced $\nu_t = 1$ BQHS,[31] or other fillings of the bilayer and monolayer systems,[32] T^* and Δ change similarly, and the unusual behaviors of T^* observed in this experiment have never been observed previously. This corresponds to the fact that the ground state of the $\nu_t = 1$ BQHS is the only system that possesses the XY symmetry among other QHSs. On this account, we believe that our results offer significant insights into the KT transition.

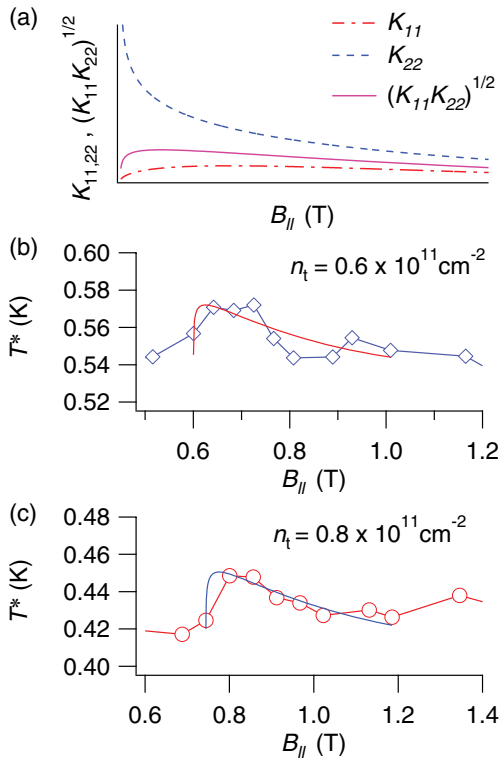

FIG. 7. (Color online) (a) Theoretically predicted values of K_{11}, K_{22}, and T_{KT} as a function of $B_\parallel$. (b) and (c) The fitting results of T^* with the theoretical T_{KT} curve of the SL phase as obtained by Read[11] for $n_t = 0.6$ and 0.8×10^{11} cm^{-2}, respectively.

V. SUMMARY

We have measured the onset temperature T^* together with the activation gap Δ in the $\nu_t = 1$ BQHS and have found interesting dependencies on n_t and $B_\parallel$. When $B_\parallel = 0$, T^* is not affected by the deterioration of electron mobility in the low-n_t regime, and it actually increases as n_t decreases, while Δ decreases in the same situation. As regards the $B_\parallel$ dependence, T^* rises at the C-IC transition point, and this is again contrary to the behavior of Δ. When examined in reference to the KT transition, the experimental results suggest that T^* represents T_{KT} for the cases of both bimeron separation and SL melting, based on the comparison with theoretical predictions.

ACKNOWLEDGMENTS

We are grateful to N. Kumada, K. Muraki, and T. Saku of the NTT Basic Research Laboratories and Y. Hirayama of Tohoku University for providing us with a high-mobility double quantum well sample and for the helpful discussions. We also acknowledge the discussions that we had with T. Arai. This research was supported in part by Grants-in-Aid for Scientific Research (No. 21340082, No. 21540254, No. 21740236, No. 22840045, and No. 24540331), a Grant for Basic Research Projects from the Sumitomo Foundation, and Grants-in-Aid for Researchers from Hyogo College of Medicine (2010 and 2011).

*terasawa@hyo-med.ac.jp

[1]Z. F. Ezawa, *Quantum Hall Effects: Field Theoretical Approach and Related Topics,* 2nd ed. (World Scientific, Singapore, 2008).
[2]S. M. Girvin and A. H. MacDonald, in *Perspectives in Quantum Hall Effects*, edited by A. Pinczuk and S. D. Sarma (Wiley, New York, 1997).
[3]M. Kellogg, J. P. Eisenstein, L. N. Pfeiffer, and K. W. West, Phys. Rev. Lett. **93**, 036801 (2004).
[4]E. Tutuc, M. Shayegan, and D. A. Huse, Phys. Rev. Lett. **93**, 036802 (2004).
[5]I. B. Spielman, J. P. Eisenstein, L. N. Pfeiffer, and K. W. West, Phys. Rev. Lett. **84**, 5808 (2000).
[6]Y. Yoon, L. Tiemann, S. Schmult, W. Dietsche, K. von Klitzing, and W. Wegscheider, Phys. Rev. Lett. **104**, 116802 (2010).
[7]L. Tiemann, Y. Yoon, W. Dietsche, K. von Klitzing, and W. Wegscheider, Phys. Rev. B **80**, 165120 (2009).
[8]J. M. Kosterlitz and D. J. Thouless, J. Phys. C **6**, 1181 (1973); *Progress in Low Temperature Physics*, edited by D. F. Brewer (North-Holland Publishing Company, Amsterdam, 1978), Chap. 5.
[9]K. Yang, K. Moon, L. Zheng, A. H. MacDonald, S. M. Girvin, D. Yoshioka, and S.-C. Zhang, Phys. Rev. Lett. **72**, 732 (1994).
[10]K. Moon, H. Mori, K. Yang, S. M. Girvin, A. H. MacDonald, L. Zheng, D. Yoshioka, and S.-C. Zhang, Phys. Rev. B **51**, 5138 (1995).
[11]N. Read, Phys. Rev. B **52**, 1926 (1995).
[12]K. Yang, K. Moon, L. Belkhir, H. Mori, S. M. Girvin, A. H. MacDonald, L. Zheng, and D. Yoshioka, Phys. Rev. B **54**, 11644 (1996).
[13]C. B. Hanna, A. H. MacDonald, and S. M. Girvin, Phys. Rev. B **63**, 125305 (2001).
[14]A. Fukuda, D. Terasawa, M. Morino, K. Iwata, S. Kozumi, N. Kumada, Y. Hirayama, Z. F. Ezawa, and A. Sawada, Phys. Rev. Lett. **100**, 016801 (2008).
[15]D. Terasawa, S. Kozumi, A. Fukuda, M. Morino, K. Iwata, N. Kumada, Y. Hirayama, Z. F. Ezawa, and A. Sawada, Phys. Rev. B **81**, 073303 (2010).
[16]S. Q. Murphy, J. P. Eisenstein, G. S. Boebinger, L. N. Pfeiffer, and K. W. West, Phys. Rev. Lett. **72**, 728 (1994).
[17]T. S. Lay, Y. W. Suen, H. C. Manoharan, X. Ying, M. B. Santos, and M. Shayegan, Phys. Rev. B **50**, 17725 (1994).
[18]M. Abolfath, R. Golestanian, and T. Jungwirth, Phys. Rev. B **61**, 4762 (2000).
[19]K. Muraki, N. Kumada, T. Saku, and Y. Hirayama, Jpn. J. Appl. Phys. **39**, 2444 (2000).
[20]M. Suzuki, A. Sawada, A. Ishiguro, and K. Maruya, Cryogenics **37**, 275 (1997).
[21]N. E. Bonesteel, I. A. McDonald, and C. Nayak, Phys. Rev. Lett. **77**, 3009 (1996).
[22]B. I. Halperin, P. A. Lee, and N. Read, Phys. Rev. B **47**, 7312 (1993); V. Kalmeyer and S.-C. Zhang, *ibid.* **46**, 9889 (1992).
[23]R. R. Du, H. L. Stormer, D. C. Tsui, L. N. Pfeiffer, and K. W. West, Phys. Rev. Lett. **70**, 2944 (1993); R. L. Willett, R. R. Ruel, K. W. West, and L. N. Pfeiffer, *ibid.* **71**, 3846 (1993); W. Kang, H. L. Stormer, L. N. Pfeiffer, K. W. Baldwin, and K. W. West, *ibid.* **71**, 3850 (1993).
[24]P. Giudici, K. Muraki, N. Kumada, and T. Fujisawa, Phys. Rev. Lett. **104**, 056802 (2010).
[25]Z. F. Ezawa, K. Ishii, and G. Tsitsishvili, Phys. E **40**, 1557 (2008).
[26]D. J. Bishop and J. D. Reppy, Phys. Rev. Lett. **40**, 1727 (1978).
[27]S. N. Coppersmith, D. S. Fisher, B. I. Halperin, P. A. Lee, and W. F. Brinkman, Phys. Rev. Lett. **46**, 549 (1981); Phys. Rev. B **25**, 349 (1982).
[28]M. E. Fisher and D. S. Fisher, Phys. Rev. B **25**, 3192 (1982).
[29]S. Park, K. Moon, C. Ahn, J. Yeo, C. Rim, and B. H. Lee, Phys. Rev. B **66**, 153318 (2002).
[30]E. Papa and A. M. Tsvelik, Phys. Rev. B **66**, 155304 (2002).
[31]A. Fukuda, D. Terasawa, T. Morikawa, Y. D. Zheng, T. Arai, Z. F. Ezawa, and A. Sawada, Proceedings of the 26th International Conference on Low Temperature Physics (LT26), J. Phys.: Conf. Ser. (to be published).
[32]See, for example, A. Usher, R. J. Nicholas, J. J. Harris, and C. T. Foxon, Phys. Rev. B **41**, 1129 (1990).